

Rotating Halos and the Microlensing MACHO Mass Estimate

Geza Gyuk¹ and Evalyn Gates^{2,3}

¹*S.I.S.S.A., via Beirut 2-4, 34014 Trieste, Italy*

²*Adler Planetarium, 1300 Lake Shore Drive, Chicago, IL 60605*

³*Department of Astronomy & Astrophysics, The University of Chicago, Chicago, IL 60637*

Received ***

ABSTRACT

We investigate the implications of a bulk rotational component of the halo velocity distribution for MACHO mass estimates. We find that for a rotating halo to yield a MACHO mass estimate significantly below that of the standard spherical case, its microlensing must be highly concentrated close to the Sun. We examine two classes of models fitting this criteria: a highly flattened $1/r^2$ halo, and a spheroid-like population with whose density falls off as $1/r^{3.5}$. The highly flattened $1/r^2$ models can decrease the implied average MACHO mass only marginally and the spheroid models not at all. Generally, rotational models cannot bring the MACHO mass implied by the current microlensing data down to the substellar range.

Key words: Galactic halo: microlensing: dark matter

1 INTRODUCTION

Recent microlensing results from the MACHO collaboration suggest that in the context of a spherical isothermal model for the Galactic halo, some significant fraction of the halo is composed of objects with masses of about $0.4M_{\odot}$ (Alcock et al. 1996). Such masses are consistent with several astrophysical candidates for MACHOs – low mass main sequence stars, white dwarfs, and black holes. Each of these candidates, however, is subject to a variety of constraints that present serious challenges for successful models in which they form a significant fraction of the halo. Low mass main sequence stars should be easily visible, and recent direct searches for these stars limit their contribution to the halo to be less than 3% (Flynn et al. 1996; Graff & Freese 1996). The limits on halo white dwarf stars are much looser. Very old white dwarfs would be cool and faint enough to have evaded direct detection thus far and yet still be present in the halo in significant numbers (Graff et al. 1997; Adams & Laughlin 1996; Chabrier et al. 1996). The progenitors of these white dwarfs presumably formed as a very early generation of stars. This scenario has its own problems, however. The progenitor stars would have produced copious amounts of metal enriched gas, which is not seen in the Galactic abundances (Hegyí et al. 1986; Gibson & Mould 1997). Ridding the Galaxy of this metal enriched gas would require a strong Galactic wind at the appropriate time (Fields et al. 1996). In addition, this scenario requires a stellar mass function for the halo stars that is peaked at a much higher mass than

is observed in the disk today. Unless the initial mass function is strongly suppressed for low masses we should still see the low mass main sequence stars that would have been produced along with the higher mass white dwarf progenitor stars (Ryu et al. 1990; Adams & Laughlin 1996). Primordial black hole candidates require a fine tuning of the initial distribution of density perturbations, although there has been some recent work on black holes formed at the QCD phase transition (Jedamzik 1997).

In this paper we explore an alternative explanation for the relatively long term event durations seen by the MACHO group. MACHO mass estimates are derived from the observed event duration, with the assumption of a model for the MACHO distribution and velocity structure. The event duration is a function not only of the mass of the lens, but also of the distance to the lens and its transverse (with respect to the line of sight) velocity. Without the additional information obtained, for example, by a parallax or binary lens event, in which case the velocity of the lensing object can sometimes be extracted and an independent estimate of the distance to the lens, the mass of an individual event cannot be determined directly. The distance along the lensing tube and transverse velocity are known only in a statistical sense (for a given model), and therefore only a statistical estimate of the mass of a population of lenses can be made. However, even given a large number of events, the mass estimate still depends strongly on the assumed distribution function (phase-space density) of the lenses. For example, MACHOs which are moving through the lensing tube with

a transverse velocity that is much less than that in a standard isothermal halo model will result in much longer event durations for a given mass.

Brown dwarf stars, with masses below $0.08M_{\odot}$, represent a less troublesome candidate for the observed microlensing events toward the Large Magellenic Cloud (LMC) but appear incompatible with the current data in the context of a standard isothermal halo model (Alcock et al. 1996). However, the viability of such lens candidates could be very different in a model with a non-standard MACHO distribution function.

In order to explore the effects of a non-standard MACHO distribution function, we allow for a bulk rotational component of the MACHO halo and anisotropic velocity dispersion. While a large bulk rotation of a spherical halo seems unlikely, there is no reason to exclude such a component *a priori*. Further, the MACHOs, which represent only about 20% – 40% of the total halo mass (Gates et al. 1997; Gates et al. 1996), may be in a more condensed or flattened distribution than the CDM halo, and thus it seems reasonable to expect some rotational component to their velocity profile.

2 MICROLENSING TOOLS

In order to compare our models to the MACHO data we first calculate the average duration. Note that we are not attempting here to determine a detailed model for the halo, in which case we would need to consider the event duration on an event-by-event basis, but rather to explore the potential of non-standard halo distribution functions to affect the MACHO mass estimate. The average event duration is directly related to the optical depth, rate and MACHO mass for a given model.

$$\bar{t}_{model} = \frac{\tau}{\Gamma}, \quad (1)$$

or

$$\bar{t}_{model} = \frac{\tau_{model}}{\Gamma_{1M_{\odot}}} \sqrt{\frac{\bar{m}}{1M_{\odot}}} \quad (2)$$

where we have now calculated the rate for solar mass MACHO's and made the mass dependence explicit. For a given model we can then extract the prediction for the average MACHO mass,

$$\frac{\bar{m}}{1M_{\odot}} = \left[\bar{t}_{obs} \frac{\Gamma_{1M_{\odot}}}{\tau_{model}} \right]^2. \quad (3)$$

Calculation of the observed average duration (Appendix A) gives a value of 61 days. Due to the low number of events and the statistics of microlensing (Han & Gould 1995), the possible error is very large. Nevertheless, for the remainder of this paper we will utilize the observed average duration: we are interested in how rotation of the halo might effect the *central* value for the MACHO mass estimate.

The optical depth towards the LMC is evaluated in the standard way,

$$\tau = \pi \int_0^{D_s} R_E^2(l) \frac{\rho(l)}{m} dl \quad (4)$$

where $R_E(l)$ is the Einstein radius at distance l ,

$$R_E(l) = \sqrt{\frac{4Gm}{c^2} \frac{l(D_s - l)}{D_s}}, \quad (5)$$

and $D_s = 50$ kpc is the distance to the source.

Calculating the microlensing rate for a moving observer and source (the microlensing tube is tumbling) in an arbitrary MACHO distribution is slightly more complex. For each segment dl of the microlensing tube we can calculate the corresponding infinitesimal contribution to the rate, $d\Gamma$. Let $f_T(v, l)$ be the distribution function of the MACHOs in the frame of the tube at location l along the tube. For every element of the velocity distribution $\Delta v_x \Delta v_y \Delta v_z$ there is a contribution to the rate,

$$\begin{aligned} \Delta^3 d\Gamma &= 2R_E(l) dl |\vec{v}_{\perp}| f_T(\vec{v}, l) \Delta v_x \Delta v_y \Delta v_z \\ &= 2R_E(l) dl |\vec{v} \times \hat{l}| f_T(\vec{v}, l) \Delta v_x \Delta v_y \Delta v_z \end{aligned} \quad (6)$$

where $2R_E(l)dl$ is the cross-section of the segment and \hat{l} is the unit vector pointing along the microlensing tube. Integrating over all velocities we have

$$\begin{aligned} d\Gamma &= 2R_E(l) dl \int_{\vec{v}} |\vec{v} \times \hat{l}| f_T(\vec{v}, l) d^3\vec{v} \\ &= 2R_E(l) dl \langle |v_{\perp}| \rangle \rho(l)/m, \end{aligned} \quad (7)$$

where $\langle |v_{\perp}| \rangle$ is the expectation value of the transverse velocity relative to the microlensing tube. Integrating along the line of sight we obtain

$$\Gamma = 2 \int_0^{D_s} R_E(l) \frac{\rho(l)}{m} \langle |v_{\perp}| \rangle dl. \quad (8)$$

It will be useful to consider the average duration due to events at a distance l from the Sun,

$$\begin{aligned} \bar{t}_{0.1}(l) &= \frac{d\tau(l)}{d\Gamma(l)} \\ &= \frac{\pi R_E(l)}{2 \langle |v_{\perp}| \rangle}, \end{aligned} \quad (9)$$

where the Einstein radius is evaluated assuming a mass of $0.1M_{\odot}$. We also consider the fractional event rate, $d\Gamma/\Gamma$, as a function of the distance l , i.e. the fraction of events that occur at any given distance.

3 EFFECT OF ROTATION

We start by examining the “standard” halo model,

$$\rho = \rho_0 \frac{r_0^2 + a^2}{r^2 + a^2} \quad (10)$$

where $a = 5$ kpc and $r_0 = 8.0$ kpc, with no rotation, flattening or anisotropy. Figure 1 shows the transverse velocity with respect to the microlensing tube as a function of distance from the Sun. The transverse velocity is largest towards the ends where the tumbling velocity due to the motion of the sun and LMC is greatest, but overall is essentially flat. Figure 2 shows the average event duration, again as a function of distance, assuming a MACHO halo composed of $0.1M_{\odot}$ objects. The duration is largest near the center and drops to zero for objects close to either end of the microlensing tube. The maximum average duration is quite low, only about 43 days. Regardless of the distribution of event distances, the average duration over the entire tube can be no larger than this. Scaling to the observed average duration of 61 days we

[htb]

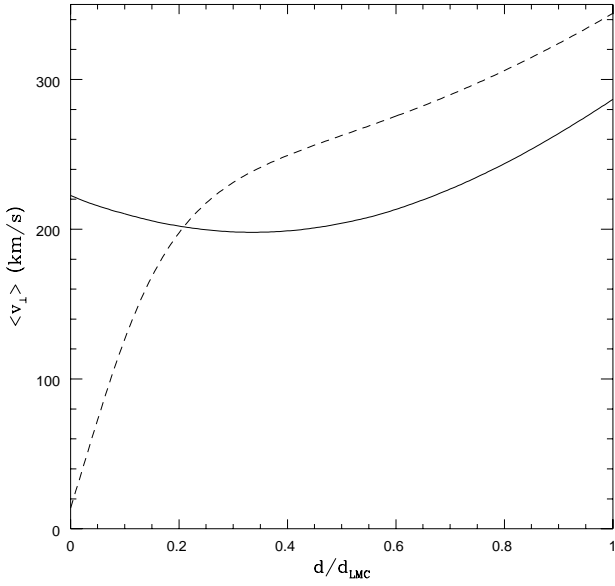


Figure 1. Transverse velocities for the “standard” (solid) and rotating (dashed) halos.

[htb]

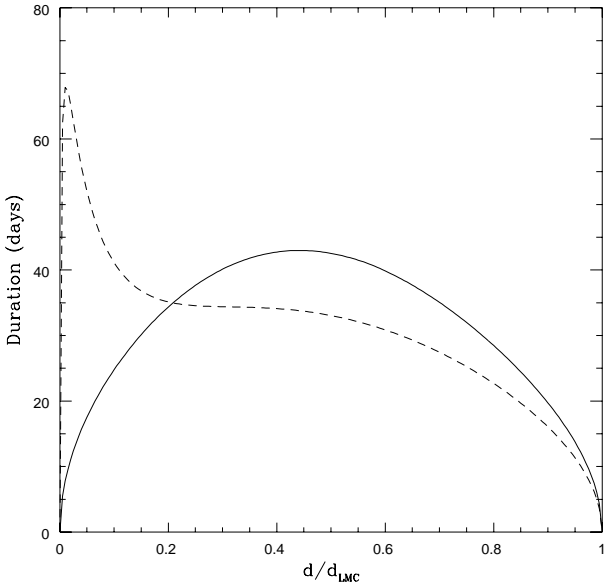


Figure 2. Average event durations assuming $0.1M_{\odot}$ MACHOs for the “standard” (solid) and rotating (dashed) halos.

find a minimum possible average mass of $0.2M_{\odot}$. The fractional event rate as a function of distance for this model is shown in Figure 3. The actual distribution of events favours the first part of the microlensing tube, where the Einstein radius is small and durations correspondingly short, leading to a much larger estimated MACHO mass, $\sim 0.4M_{\odot}$. Since the transverse velocity is relatively flat over the entire distance to the LMC, this distribution is driven mainly by the distribution of the lenses.

[htb]

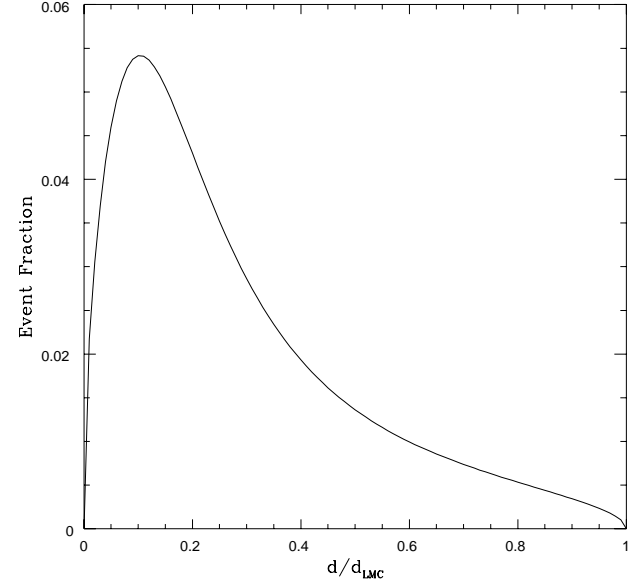


Figure 3. Distribution of the event distances for the “standard” halo.

Next, for comparison, we consider an extreme model – an idealized cold co-rotating halo ($v_{\text{rot}}=220$ km/s) model with zero velocity dispersion (even in the z-direction). While obviously not a realistic model, it does allow us to examine the limits on MACHO mass estimate reduction in models with a rotational component for the halo velocity structure. Figure 1 shows the average transverse velocity of this model as a dashed line. As expected, the transverse velocity close to the observer is low. However, note that the transverse velocity at more distant points is actually quite high: the MACHOs sweep past the microlensing tube because the LMC velocity is not aligned with the rotation of the Milky Way as is the motion of the Sun. The dashed line in Figure 2 is the average duration of events (for $0.1M_{\odot}$ MACHOs) for the co-rotating halo model. We see a dramatic effect due to the reduced velocities close to the Sun: there is a sharp peak in the durations of events at very small distances. In general, the durations are increased for distances smaller than 10 kpc and decreased for distances greater than 10 kpc, reflecting the relative velocities at these distances. There is a small region where the durations are above 61 days, the observed average duration. This implies that it is possible, at least in principle, to obtain average durations matching those observed with $0.1M_{\odot}$ MACHOs, and suggests distributions which are highly concentrated toward the center of the Galaxy as the most likely way to achieve this.

If a rotating halo is to lead to reduced mass prediction for the MACHOs, essentially all the lensing must occur very close to the observer. The distribution from the standard model is too wide and peaks at too large a value to fully sample the initial peak in average event duration due to rotation. Any benefit from the increased durations at short distance will be offset by the decreased durations at larger distances. We consider two options for bringing the microlensing closer to home: a density fall-off faster than

$1/r^2$ or a flattened halo. Both of these possibilities are quite reasonable. The stellar halo population we *do* know about, the spheroid, has a density distribution that falls off roughly as $1/r^{3.5}$. The MACHO halo may trace this distribution. On the other hand, various observations (Olling 1996; Sackett et al. 1994) suggest that dark halos are flattened, and simulations consistently show that the CDM halos generically form with departures from spherical symmetry. The dissipative baryonic component of the halo, the MACHOs, might be expected to be even further from spherical. We know of at least one component of the Galaxy, the disk, that became significantly flattened before forming stars. In the following section we examine these models in detail.

4 MODELING

Following the above discussion, we will consider three density profiles:

an isothermal halo model with core radius a

$$\rho = \rho_0 \frac{r_0^2 + a^2}{r^2 + a^2}, \quad (11)$$

a flattened (axis ratio $q=0.2$) inverse square halo ^{*}

$$\rho = \rho_0 \frac{r_0^2 + a^2}{R^2 + z^2/q^2 + a^2}, \quad (12)$$

and a spheroid-like halo

$$\rho = \rho_0 \frac{r_0^{3.5} + a^{3.5}}{r^{3.5} + a^{3.5}}. \quad (13)$$

We fix the core radii at $a = 5$ kpc for the $1/r^2$ models and $a = 1$ kpc for the spheroid model. (We examined the effects of varying the core radius for all 3 models and found them to be unimportant to our final results.)

To estimate the MACHO mass implied by these models, we need to specify not only the density distribution, but also the velocity structure of the halo. We assume that the phase space distribution is a simple anisotropic gaussian, offset from the origin by the rotation velocity and aligned at each point with cylindrical Galactic coordinates. [†] We do not attempt to construct completely “self-consistent” halo models. For the flattened or centrally condensed halos we consider, such models would need to incorporate the bulge and disk, as well as halo self-consistency. This is presently well beyond the state of the art given the large uncertainties in essentially all Galactic parameters. Furthermore, microlensing constraints are sufficiently weak (due to low number of events) that such sophistication is unwarranted at present.

* We considered using an Evans model for the halo since these come with a consistent prescription for the phase space density. However such models cannot produce a halo as flattened as we wished to explore, at most obtaining an equivalent flattening in the density of $\approx 1/3$.

[†] Most of the lensing in our models takes place close to the Solar position, where a velocity ellipsoid aligned with Galactic cylindrical coordinates is a reasonable approximation, and over a relatively narrow range in distance where the anisotropic velocity dispersions should not change radically. Thus, while these are not the most general set of assumptions, they are sufficient for our purposes and greatly simplify the calculations.

The Jeans equations for the above time-independent distributions simplify to,

$$\frac{\partial(\rho \overline{v_R^2})}{\partial R} + \frac{\rho}{R}(\overline{v_R^2} - \overline{v_\phi^2}) + \rho \frac{\partial \Phi}{\partial R} = 0 \quad (14)$$

$$\frac{\partial(\rho \overline{v_z^2})}{\partial z} + \rho \frac{\partial \Phi}{\partial z} = 0, \quad (15)$$

where Φ is the potential of the total halo. We further assume that $\frac{\partial \overline{v_R^2}}{\partial R} \approx 0$ and $\frac{\partial \overline{v_z^2}}{\partial z} \approx 0$ at points in the halo of interest for this work. Although this is probably a poor assumption for detailed modeling, we accept it in order to focus on the effects of *rotation* on the microlensing mass estimates. We then have

$$\begin{aligned} \left(-\frac{\partial \ln \rho}{\partial \ln R} - 1\right) \sigma_R^2 + \sigma_\phi^2 + \overline{v_\phi^2} &= R \frac{\partial \Phi}{\partial R} \\ \left(\frac{\partial \rho}{\partial z}\right) \sigma_z^2 &= -\rho \frac{\partial \Phi}{\partial z} \end{aligned} \quad (16)$$

where $\sigma_R^2 = \overline{v_R^2}$, $\sigma_z^2 = \overline{v_z^2}$ and $\sigma_\phi^2 + \overline{v_\phi^2} = \overline{v_\phi^2}$ (breaking it up into random and bulk flows). The derivative $\frac{\partial \Phi}{\partial R}$ is just the R-component of the force at R. Since we are roughly at the equator, $R \frac{\partial \Phi}{\partial R}$ is simply the square of the circular velocity at R, $v_c^2(R) \approx (220 \text{ km/s})^2$

To complete this set of equations we need to find $\frac{\partial \Phi}{\partial z}$. We assume that the bulk of the halo, and thus the major contribution to the potential, comes from the non-baryonic component, whose distribution is assumed to be that of equation 12, with core radius $a_{\text{NB}} = 0$ and arbitrary flattening q_{NB} independent of the MACHO halo. It can be shown (Appendix B) that to first order in z

$$\frac{\partial \Phi}{\partial z} = v_c^2 \left[\sqrt{\frac{q_{\text{NB}}^2}{1 - q_{\text{NB}}^2}} \sin^{-1} \sqrt{1 - q_{\text{NB}}^2} \right]^{-1} \frac{z}{R^2} \quad (17)$$

near the equatorial plane. This gives

$$\sigma_z^2 = -\rho v_c^2 \left[\sqrt{\frac{q_{\text{NB}}^2}{1 - q_{\text{NB}}^2}} \sin^{-1} \sqrt{1 - q_{\text{NB}}^2} \right]^{-1} \frac{z}{R^2} \left(\frac{\partial \rho}{\partial z}\right)^{-1}. \quad (18)$$

The lowest value for σ_z^2 is obtained for a spherical ($q=1.0$) non-baryonic halo. A larger value of the vertical velocity dispersion will drive the transverse velocities up, the event durations down, and ultimately yield a higher mass estimate. Since we are interested here in models which lower the MACHO mass estimates we take $q_{\text{NB}} = 1$ and find

$$\begin{aligned} \left(-\frac{\partial \ln \rho}{\partial \ln R} - 1\right) \sigma_R^2 + \sigma_\phi^2 + \overline{v_\phi^2} &= v_c^2 \\ \left(\frac{\partial \rho}{\partial z}\right) \sigma_z^2 &= -\rho v_c^2 \frac{z}{R^2} \end{aligned} \quad (19)$$

As we will see, the precise form of the relationship between the rotation and velocity dispersion is not important for our conclusions. We use equation 19 as a general guide to which combinations of rotation and velocity dispersions are reasonable.

5 RESULTS AND DISCUSSION

We plot our results for the various halo models in figures 4 through 6. The solid contours correspond to the predicted MACHO mass estimate, corresponding to the average MACHO event duration of 61 days, as a function of the

[htb]

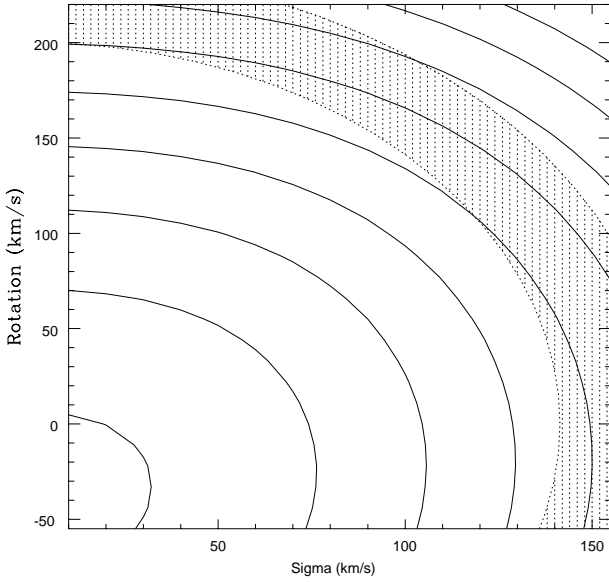


Figure 4. Average MACHO mass for an isothermal halo based on the MACHO collaboration average event duration. Countours are 0.15, 0.2, 0.25, 0.3,... M_{\odot} from left side.

(one-dimensional) velocity dispersion \ddagger and rotation speed. For reference, the standard non-rotating halo with isotropic maxwellian velocity dispersion has a one-dimensional dispersion $\sigma = 156\text{km/s}$.

The models within $\pm 10\%$ of our $\sigma - v_{\text{rot}}$ curve (equation 19) lie in the shaded region between the dotted lines. Models below this region are unlikely to have sufficient support. The trade-off of dispersion velocity for rotation velocity can be seen clearly.

Figures 4, 5 and 6 show the predicted MACHO masses for the spherical $1/r^2$, flattened $1/r^2$ and spherical $1/r^{3.5}$ halo models. In no case does the predicted mass for the current MACHO event duration go below $0.25M_{\odot}$ in the allowed region indicated by equation 19. As expected following the discussion in section 3, the spherical $1/r^2$ model actually predicts increasing MACHO mass estimates as it becomes more rotation supported. Rotation increases the velocities along the microlensing tube far from the Sun leading to shorter event durations for a given MACHO mass, or conversely, a larger MACHO mass estimate for a given observed event duration. Most microlensing in the standard halo model occurs at distances where the velocities are increased when a rotational velocity component is added and hence the mass estimates for a given event duration increase.

In contrast, in highly flattened $1/r^2$ halo models rotation does lead to reduced mass estimates. However, the improvement is not as dramatic as might be hoped. The reason is a little subtle. In the absence of rotation, the microlensing is concentrated in the first part of the tube by the flattening

\ddagger In the discussion that follows we take $\sigma = \sigma_R = \sigma_{\phi}$. We have also considered models with a constant anisotropy $\sigma_R = \alpha\sigma_{\phi}$, where $0.3 \leq \alpha \leq 3.0$; our results are essentially unchanged for these models.

[htb]

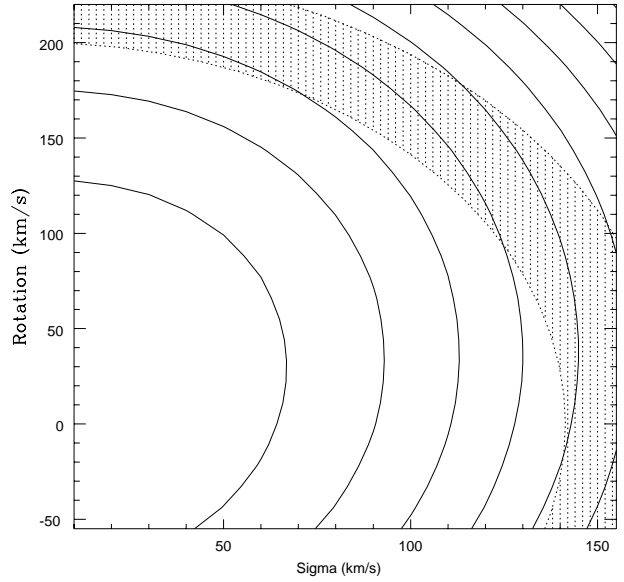


Figure 5. Same as Figure 4 for the flattened $1/r^2$ halo. Countours are 0.15, 0.2, 0.25, 0.3,... M_{\odot} from left side.

of the halo. We can see that predicted mass estimates for the flattened halo model with no rotation are a little higher than for the spherical model since in this region the durations for the non-rotating model are short. However, the fractional rate is also dependent on the average transverse velocity of MACHOs. Because a flattened halo has a lower z-velocity dispersion, when rotation is added the transverse velocity can become very low close to the observer. This is precisely why rotation might be expected to lower the predicted MACHO mass estimates. However, the low transverse velocity also suppresses the event rate close to the observer and shifts the distribution of events to larger distances where the transverse velocities are higher. These two effects compete, with the end result that the reduction to the MACHO mass estimate due to rotation is only modest.

Our second hope for taking advantage of rotation, a more concentrated $1/r^{3.5}$ spheroid, is also disappointing. Supporting a spheroidal halo rotationally leads to very little change in the MACHO mass estimate. Rotation fails to reduce the mass estimates in the spheroidal case for reasons slightly different than those for the flattened halo. For a spheroidal MACHO distribution, transverse velocities never get very low, even close to the observer. Hence, little benefit is derived from the central concentration. Such a spheroidal model also has serious difficulties producing a high optical depth without ruining the flatness of the Galactic rotation curve.

In this section we have explored three general classes of halo models, which have been unable, even with the additional of a generous rotational component, to reduce the MACHO mass estimates for the current observed event durations to masses in the substellar regime. The failure of rotating halos to significantly reduce MACHO mass estimates can be summed up as follows. First, the virial theorem implies that a typical velocity for a particle in an extended halo

[htb]

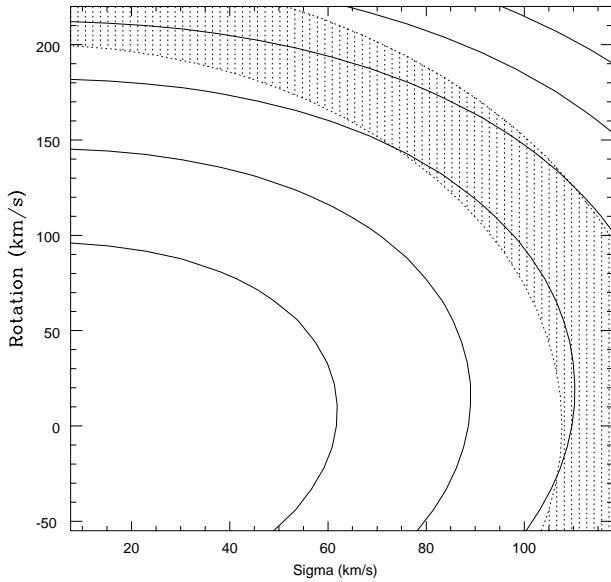


Figure 6. Same as Figure 4 for the spheroidal halo. Countours are 0.2, 0.25, 0.3,... M_{\odot} from left side.

will be roughly the same regardless of whether the halo is or is not rotationally supported. Velocities cannot be made arbitrarily low. Secondly, the direction to the LMC is “awkward”, that is, it respects none of the symmetries of the Galaxy. This has several implications for attempts to lower the MACHO mass estimates. Bulk velocities due to rotation cannot be used to cancel out some of the motion of the MACHOS through the lensing tube except possibly very close to the observer. An effort to concentrate the MACHOs in this region, however, is self-defeating in the models we explored. The event rate in such models is dominated by MACHOs moving through the tube further away from the observer, and the net effect on the MACHO mass estimate is not sufficiently large to reach the substellar regime with current data. Further, the direction of the LMC makes it impossible to arrange, in any natural way, an anisotropic velocity dispersion such that the net transverse velocity through the tube is significantly reduced (Gyuk & Gates in preparation 1997).

6 CONCLUSIONS

Scenarios in which brown dwarfs populate a standard spherical, non-rotating halo in significant numbers predict event durations significantly (more than a factor of 2) shorter than observed in the current MACHO data. We have explored halo models with a bulk rotational component in an attempt to lower the predicted mass estimate for the MACHO events to the substellar regime. We find that unless essentially *all* of the lensing takes place within 1-2 kpc of the Sun *and* residual velocity dispersions are very low, $\lesssim 30\text{km/s}$, it is not possible to reduce the MACHO mass estimate in these models to the brown dwarf mass range. Such a configuration no longer resembles a halo distribution for the MACHOs.

A highly flattened rotating halo was our most successful

model in reducing MACHO mass estimates, although even this model did not reduce the microlensing mass estimate below about $0.25M_{\odot}$. This suggests that a thick disk configuration with a steeper (exponential) density fall off away from the Galactic plane might be able to reduce the mass estimates further. A high rotation velocity is also more natural for such a distribution than for a more extended halo. Preliminary work shows that a thick disk can indeed reduce the mass estimate, but only to around $0.15 - 0.2M_{\odot}$. We will report on this in more detail in a forthcoming paper.

In summary, the prospect for a brown dwarf microlensing halo appears dim given the current data, and the question of what and where the MACHO lenses are remains unanswered.

REFERENCES

- Adams F.C., Laughlin G., 1996, ApJ, 468, 586
 Alcock C. et al., 1996 sub to ApJ (astro-ph/9606165)
 Binney J., Tremaine S., *Galactic Dynamics* (Princeton University Press, Princeton, 1987).
 Chabrier G., Segretain L., Mera D., 1996, (astro-ph/9606083)
 Fields B.D., Mathews G.J., Schramm D.N., 1996, (astro-ph/9606011)
 Flynn C., Gould A., Bahcall J., 1996, ApJ, 466, L55
 Gates E., Gyuk G., Turner M.S., 1997, Proceedings of the 18th Texas Symposium on Relativistic Astrophysics, eds. A. Olinto, J. Frieman and D.Schramm (World Scientific, Singapore, 1997).
 Gates E., Gyuk G., Turner M.S., 1996, Phys. Rev. D, 53, 4138
 Gibson B. K., Mould J. R., 1997, ApJ, in press
 Graff D. S., Freese K., 1996, ApJ, 467, L65
 Graff D. S., Laughlin D., Freese K., 1997, (astro-ph/9704125)
 Gyuk G., Gates E., 1997, in preparation
 Han C. & Gould A., 1995, ApJ, 449, 521
 Hegyi D. J., Olive K.A., 1986, ApJ, 303, 56
 Jedamzik K., 1997, Phys. Rev. D, in press (astro-ph/9605152)
 Olling R. P., 1996, AJ, 112, 481
 Ryu D., Olive K.A., Silk J., 1990, ApJ, 353, 81
 Sackett P., Rix H., Jarvis B.J., Freeman K.C., 1994, ApJ, 436, 629

APPENDIX A : CALCULATION OF AVERAGE EVENT DURATION

From the observed events we can construct the *observed* distribution function of time scales, $\nu(\hat{t})$. The true distribution will then be $\rho(\hat{t}) = \nu(\hat{t})/\epsilon(\hat{t}) / \int \nu(\hat{t})/\epsilon(\hat{t})d\hat{t}$. We want to calculate

$$\bar{\hat{t}} = \int \hat{t}\rho(\hat{t})d\hat{t} \quad (20)$$

$$= \frac{\int \hat{t}\nu(\hat{t})/\epsilon(\hat{t})d\hat{t}}{\int \nu(\hat{t})/\epsilon(\hat{t})d\hat{t}} \quad (21)$$

which requires knowing the function $\nu(\hat{t})$. Our best guess for this will be to let

$$\nu(\hat{t}) = \frac{1}{n} \sum_i \delta(\hat{t}_i - \hat{t}). \quad (22)$$

Substituting in gives

$$\bar{t} = \frac{\sum_i \frac{t_i}{\epsilon(t_i)}}{\sum_i \frac{1}{\epsilon(t_i)}}. \quad (23)$$

Using the events and efficiencies towards the LMC (Alcock et al. 1996) we obtain $\bar{t} = 61$ days.

APPENDIX B : VERTICAL POTENTIAL

Following (Binney & Tremaine 1987), the z -component of the gravitational force generated by a density distribution $\rho = \rho(m^2)$ where $m^2 = R^2 + z^2/q^2$, is given by

$$-\frac{\partial\Phi}{\partial z} = 4\pi G \sqrt{1-e^2} \int_0^R \frac{\rho(m^2)z dm}{m[\frac{R^2}{m^2} - (1-q^2)]^{3/2}}, \quad (24)$$

where we keep only the leading order term in z , in order to obtain a lower limit on the estimate for σ_z .

Assuming a density $\rho = \rho_0 m_0^2/m^2$ we then arrive at

$$-\frac{\partial\Phi}{\partial z} = 4\pi G \frac{\rho_0 m_0^2 z}{R^2} \quad (25)$$

Rewriting this in terms of the circular velocity and flattening we find

$$\frac{\partial\Phi}{\partial z} = \frac{v_c^2}{\sqrt{q^2/(1-q^2)} \sin^{-1}(1-q^2)} \frac{z}{R^2}. \quad (26)$$

